Proceedings of the ASME 2010 3rd Joint US-European Fluids Engineering Summer Meeting and 8th International Conference on Nanochannels, Microchannels, and Minichannels
FEDSM-ICNMM2010
August 1-5, 2010, Montreal, Canada

FEDSM-ICNMM2010-30434

ANALYSIS OF CAVITATION SURGE CONSIDERING THE ACOUSTIC EFFECT OF THE INLET LINE IN A ROCKET ENGINE TURBOPUMP

Hideaki NANRI
Japan Aerospace Exploration Agency
1 Koganezawa, Kimigaya, Kakuda
Miyagi 981-1525, Japan

Naoki TANI
Japan Aerospace Exploration Agency
2-1-1 Sengen,Tsukuba
Ibaraki 305-8505, Japan

Hiroki KANNAN
Japan Aerospace Exploration Agency
1 Koganezawa, Kimigaya, Kakuda
Miyagi 981-1525, Japan

Yoshiki YOSHIDA
Japan Aerospace Exploration Agency
1 Koganezawa, Kimigaya, Kakuda
Miyagi 981-1525, Japan

ABSTRACT

In a liquid rocket engine, cavitation in an inducer of a turbopump sometimes causes instability phenomena when the inducer is operated at low inlet pressure. Cavitation surge (auto-oscillation), one such instability phenomenon, has been discussed mainly based on an inertia model assuming incompressible flow. By using this model, the frequency of the cavitation surge decreases as the inlet pressure decreases. However, we obtained interesting experimental results in which the cavitation surge frequency varied disconnectedly. Therefore, we considered the factor of fluid compression employed one-dimensional analysis applying an acoustic model, combining the inlet pipe with the sonic velocity of liquid oxygen. Consequently, the analytical results qualitatively corresponded with the experimental results. In addition, an actual liquid rocket propulsion system is usually equipped with a Pogo suppression device (PSD), which is a kind of accumulator with a hydraulic compliance, upstream of a liquid oxidizer turbopump. We modified the analytical model to include the effect of this PSD and compared the analytical results with the experimental results. It was found that the frequency of cavitation surge basically became the Helmholtz frequency, defined by the cavitation compliance and the length of pipe between the PSD and the turbopump. And when the frequency of cavitation surge coincided with one of the acoustic resonance frequencies of the inlet pipe, the cavitation surge was strongly excited.

INTRODUCTION

Launch vehicles are designed to minimize their dry mass in order to obtain better performance. As propellant tanks are major components of a rocket, decreasing their weight is a very effective way of reducing dry mass. Decreasing the pressure in a tank allows for thinner tank walls, which contributes to the efficiency of a rocket system. On the other hand, when the pressure in the tank is decreased, the inlet pressure to the turbopump of the rocket engine is decreased and the resultant cavitation in the turbopump inducer causes cavitation instabilities. Cavitation surge (auto-oscillation), i.e., one type of cavitation instability, is caused not only by the unsteady characteristic of cavitation, but by the integrated characteristics of the tank, feed pipes, valves, accumulator and cavitation.

Cavitation surge was studied in the 1960s in relation to Pogo instability, which is caused by the interaction between a rocket structure and a rocket propulsion system (Rubin [1]) . With regard to the characteristic of the turbopump, the dynamic transfer function of the inducer has been investigated to evaluate the stability (Brennen and Acosta [2]). The pump system, including tank, pipes, pump and valves, has been modeled, and the stability of the system has been evaluated (Greitzer [3]). There are several types of instabilities in turbomachines, i.e., surge, rotating stall, cavitation surge and rotating cavitation, and the unified numerical mode of these instabilities has been examined and presented (Tsujimoto et al. [4]). In these studies, however, the dynamic behavior of pressure fluctuation was evaluated mainly by the equation of continuity on the supposition that the fluid was "incompressible." The unsteady characteristic of cavitation was expressed by a mass flow gain factor (M) and cavitation compliance (K), and then the frequency of pressure oscillation was in inverse proportion to the square root of cavitation compliance (K) and the length of the inlet pipe ($1/(\rho KL/A)^{1/2}$)

(Yamamoto [5]). When the inlet pressure decreases, cavitation compliance (K) becomes large and the natural frequency of the cavitation surge is expected to decrease continuously. However, when an experimental turbopump was tested, we found that the frequency of cavitation surge changed disconnectedly as the inlet pressure decreased. This phenomenon means to be similar to acoustic resonance, which consists of a fundamental and its multiple frequencies (Chen et al. [6]). In the present paper, which is aimed at explaining the disconnection of cavitation surge frequency, we conducted simple one-dimensional analyses with an acoustic model, combining the inlet line with the sonic velocity of liquid oxygen.

NOMENCLATURE

A	=	area of inlet pipe [m^2]
c	=	speed of sound [m/s]
D	=	diameter of inlet pipe [m]
f_r	=	coefficient of friction
j	=	imaginary unit $(-1)^{1/2}$
K	=	cavitation compliance [m^4 s^2/kg]
K_{drag}	=	coefficient of friction in the inlet pipe $= f_r\, U/D$ [1/s]
K_{dragV}	=	coefficient of friction in the valve $= \Delta p/\rho UL$ [1/s]
K_{drag_PSD}	=	coefficient of friction in the PSD $= \Delta p/\rho UL$ [1/s]
L	=	length [m]
M	=	mass flow gain factor [m^3 s/kg]
n	=	an integral number
p	=	pressure [Pa]
p_1	=	pressure in the inlet of the inducer [Pa]
p_s	=	steady part of pressure [Pa]
p_u	=	unsteady part of pressure [Pa]
p_v	=	pressure of a saturated vapor [Pa]
q	=	mass flow rate [kg/s]
R	=	radius of inducer [m]
t	=	time [s]
U	=	average velocity [m/s]
u	=	velocity [m/s]
u_s	=	steady part of velocity [m/s]
u_u	=	unsteady part of velocity [m/s]
V_C	=	cavity volume [m^3]
β	=	complex frequency
σ	=	cavitation number $(= (p_1 - p_v) / \{\rho(U^2+(2\pi R\Omega)^2)\}$
σ_D	=	cavitation number at 5% head drop
ρ	=	density [kg/m^3]
Ω	=	rotational speed of turbopump [1/s]
ω	=	complex frequency $= \omega_R + j\omega_I$
ω_f	=	fundamental frequency of acoustic resonance in inlet pipe $= 2\,\pi\, c\,/\,L$ [rad/s]
ω_I	=	imaginary part of complex frequency [rad/s]
ω_R	=	real part of complex frequency [rad/s]

EXPERIMENTAL RESULTS AND ANALYTICAL MODEL

Experimental Results

Experiments on a turbopump were carried out in the high-pressure liquid oxygen turbopump test facility (Fig. 1) at the Kakuda Space Center of the Japan Aerospace Exploration Agency (JAXA). At this facility, fluid is fed from a run tank of 10 m^3 volume to a turbopump through a straight pipe with a valve that is about 10 m long. The fluid, delivered by the turbopump, is fed into a catch tank through pipes, flow meters, and flow control valves. The cavitation number (σ) can be controlled by decreasing the pressure in the run tank during a test. Figure 2(a) shows a typical FFT analysis of the inlet pressure fluctuation. According to the inertia model, when the cavitation number decreases, the frequency is expected to be decreased continuously, as indicated by the red line in Fig. 2(b). However, the present test data varied disconnectedly.

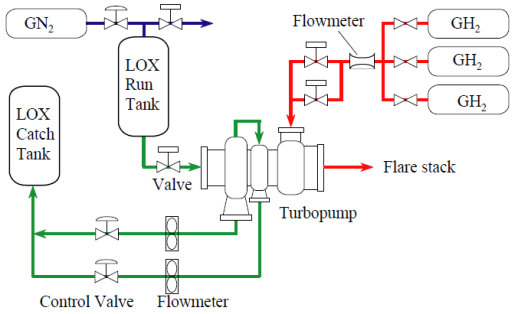

Figure 1 SCHEMATIC DIAGRAM OF TURBOPUMP TEST FACILITY

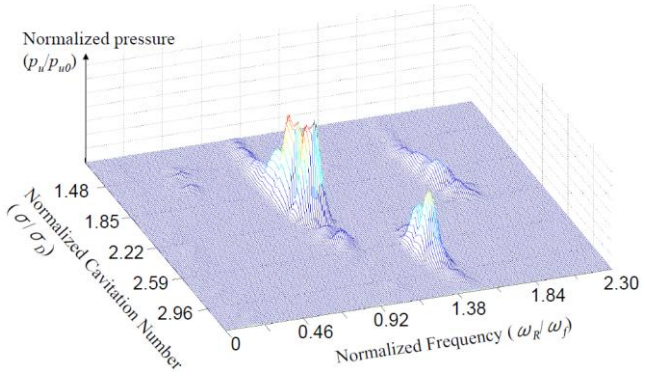

Figure 2(a) FFT ANALYSES OF PRESSURE FLUCTUATION AT INLET OF THE TURBOPUMP

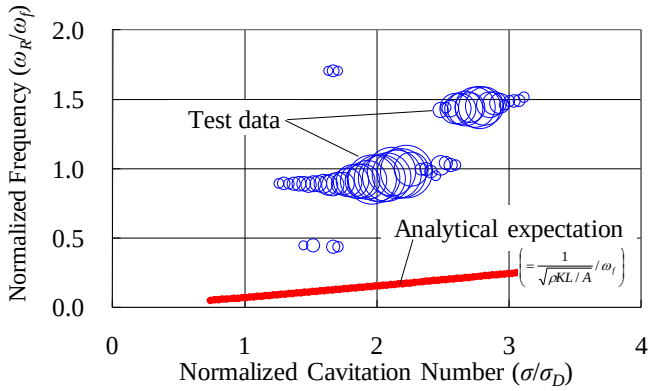

Figure 2(b) ANALYTICAL EXPECTATION BY INERTIA MODEL AND EXPERIMENAL RESULTS OF PRESSURE FLUCTUATION AT INLET TURBOPUMP. (THE SIZE OF THE BUBBLE IS THE AMPLITUDE OF THE PRESSURE FLUCTUATION)

Analytical Model

This phenomenon seems to be similar to acoustic resonance, which consists of a fundamental and its harmonic frequencies. Then we supposed that the fluid was "compressible" and conducted simple one-dimensional analyses with an acoustic model, combining the inlet pipe with the sonic velocity of liquid oxygen. The simple analytical model consists of a tank, an inlet pipe and a turbopump, as shown in Fig. 3. We simplified the model by omitting small branches in the inlet pipe and fluctuations of flow rate in the discharge pipe of the turbopump. Although an element of volume is usually applied in the discharge pipe, it is disregarded in this model because the cavity volume in the turbopump has a volume to some extent. This assumption also means that a dynamic gain of a turbopump can be omitted for simpler equations.

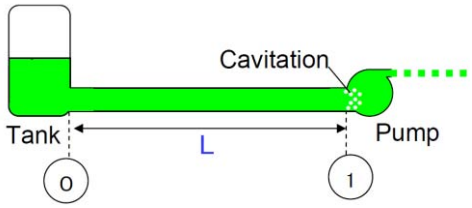

Figure 3 SIMPLE ANALYTICAL MODEL

Supposing that the fluid is compressible, we can write an acoustic wave equation as Eq. (1), where K_{drag} is the friction coefficient defined as (f_r U / D). The value for the speed of sound (c) is corrected with the diameter and the thickness of the pipe and its elasticity coefficient.

$$\frac{\partial^2 p}{\partial t^2} + K_{drag}\frac{\partial p}{\partial t} = c^2\frac{\partial^2 p}{\partial x^2} \tag{1}$$

For stability analyses, we separate pressure and velocity into steady and unsteady components: $p=p_s+p_u$ and $u=u_s+u_u$. The absolute value of the steady part is supposed to be larger than the unsteady part (p_u << p_s, u_u << u_s). Then general solutions for p_u and u_u are obtained, and if the amplitude of pressure fluctuation at the exit of the run tank is zero, the correlation between p_u and u_u at the inlet of the turbopump is written as

$$p_{u1} = -j\rho c\frac{\sqrt{\omega^2 - K_{drag}\omega j}}{\omega}\tan\left(\frac{L}{c}\sqrt{\omega^2 - K_{drag}\omega j}\right)u_{u1} \tag{2}$$

Furthermore, the equation of continuity in the turbopump can be presented as Eq. (3) using cavitation compliance (K) and mass flow gain factor (M) as unsteady cavitation characteristics.

$$K = -\left(\frac{\partial Vc}{\partial p}\right) \quad M = -\left(\frac{\partial Vc}{\partial q}\right)$$
$$u_{u1}A = K\dot{p}_{u1} + M\rho A\dot{u}_{u1} \tag{3}$$

The p_{u1} is eliminated by Eq. (2) and Eq. (3), and then the differential equation on u_{u1} is obtained.

$$u_{u1}A = \left[K\left\{-j\rho c\frac{\sqrt{\omega^2 - K_{drag}\omega j}}{\omega}\tan\left(\frac{L}{c}\sqrt{\omega^2 - K_{drag}\omega j}\right)\right\} + M\rho A\right]\dot{u}_{u1} \tag{4}$$

When the velocity u_{u1} is a sinusoidal oscillation, u_1 can be expressed as $e^{j\omega t}$. Then Eq. (4) is replaced by Eq. (5).

$$A = \left[K\left\{-j\rho c\frac{\sqrt{\omega^2 - K_{drag}\omega j}}{\omega}\tan\left(\frac{L}{a}\sqrt{\omega^2 - K_{drag}\omega j}\right)\right\} + M\rho A\right]j\omega \tag{5}$$

From this characteristic equation, the solutions of the complex frequency ($\omega=\omega_R+j\omega_I$) can be obtained. There are many solutions because Eq. (5) has a tangential function. However, we only discuss solutions within a few harmonic overtones because the purpose of this model is to verify the experimental results as shown in Fig. 2.

To calculate this analytical model under test conditions, values for cavitation compliance (K) and mass flow gain factor (M) of the turbopump as input parameters are needed. Therefore steady-state computational fluid dynamics (CFD) analyses on the inducer were conducted to obtain these values. The difference of the cavity volume in an inducer under conditions of different cavitation numbers can be obtained by steady-state CFD analyses. Consequently, the quasi-steady value for cavitation compliance (K) is calculated as shown in Fig. 4 and the analytical result of cavitation compliance (K) seem approximately inversely proportional to the cavitation number. In the same way, the differences of the cavity volume under conditions of different flow rates can be obtained by steady-state CFD analyses and the quasi-steady value for mass flow gain factor (M) is calculated as shown in Fig.4. This method was presented by Tani and Yamanishi [7].

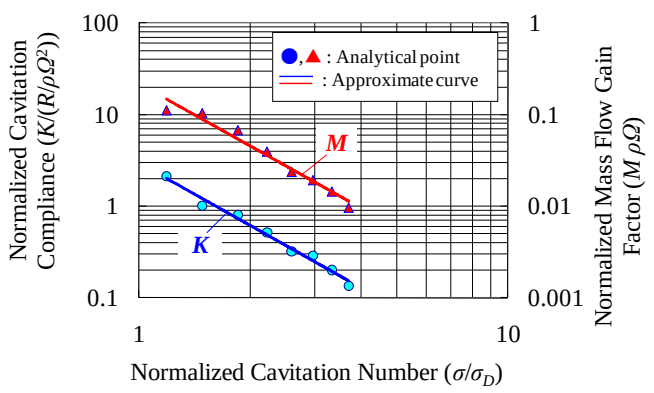

Figure 4 CAVITATION CHARACTERISTICS (*K* AND *M*) OBTAINED WITH QUASI-STEADY STATE CFD ANALYSES

ANALYTICAL RESULTS AND DISCUSSION

A comparison between the experimental results and the analytical results, using quasi-steady cavitation compliance (*K*) and mass flow gain factor (*M*), is shown in Fig. 5(a). The solutions of the analysis consist of harmonic frequencies of acoustic resonance in the inlet pipe, and the agreement between the analytical results and the experiments is fairly good. Furthermore, the frequency of the cavitation surge slightly decreased with the decrease in the cavitation number in the analytical and experimental results. Figure 6 shows the solutions of the complex frequency when cavitation compliance (*K*) is treated as a parameter. The frequency (ω_R) is slightly decreased along with the decrease in cavitation compliance (*K*). When cavitation compliance (*K*) is small, the inlet pipe has an open boundary condition on the tank side and a closed boundary condition on the turbopump side. Therefore the frequency becomes close to (2*n*+1)/4 times the fundamental frequency. On the other hand, when cavitation compliance (*K*) is large, the frequency becomes close to *n*/2 times. In other words, as the inlet pressure decreases, the characteristic of the turbopump changes from a closed boundary condition to an open boundary condition, and the frequency of the surge slightly decreases. In this way, the operating turbopump performs as an intermediate boundary condition between an open and a closed boundary because of the characteristic of the cavitation compliance (*K*), as shown in Fig. 7. Further, the Helmholtz frequency obtained by the cavitation compliance (*K*) of the inducer and the length of pipe (*L*) is plotted as a red broken line in Fig. 6(a). It is found that the 1/4 wavelength fluctuation, i.e., the fundamental frequency, becomes asymptotical to the inertia-based movement as the cavitation compliance increases.

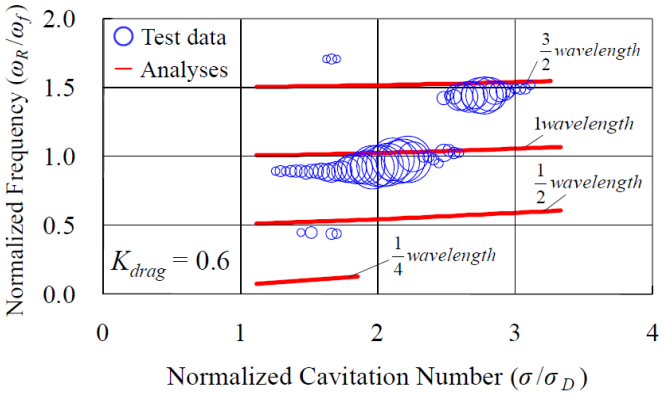

Figure 5(a) COMPARISON OF FREQUENCY BETWEEN EXPERIMENTAL RESULTS AND ANALYTICAL RESUTLS (ω_R) USING CFD-CALCULATED *K* AND *M*

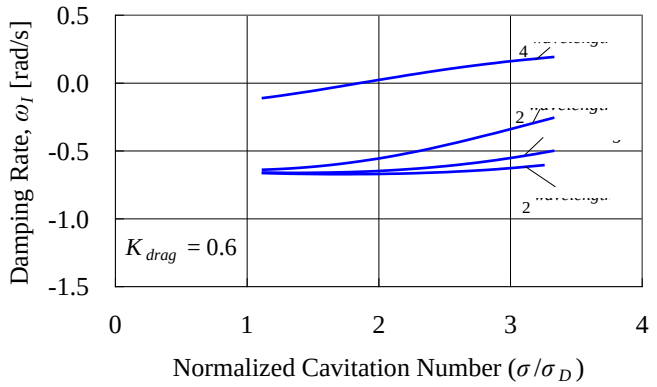

Figure 5(b) ANALYTICAL RESULTS OF DAMPING RATE (ω_I) USING K_{drag}, CFD-CALCULATED *K* AND *M*

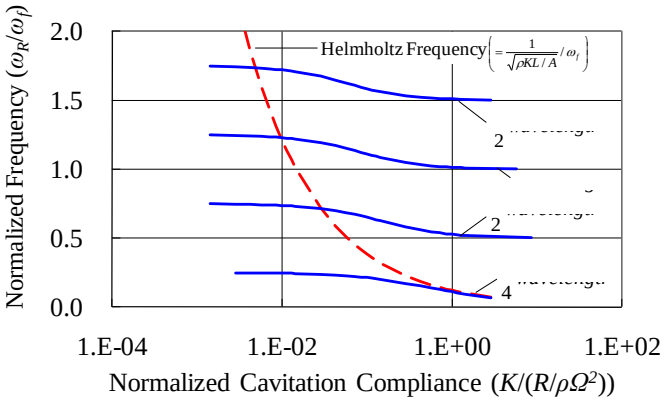

Figure 6(a) ANALYTICAL RESULTS OF THE REAL PART, ω_R, SHOWING TREND ANALYSES ON *K* ($M\rho\Omega$ = 0.035, K_{drag}= 0)

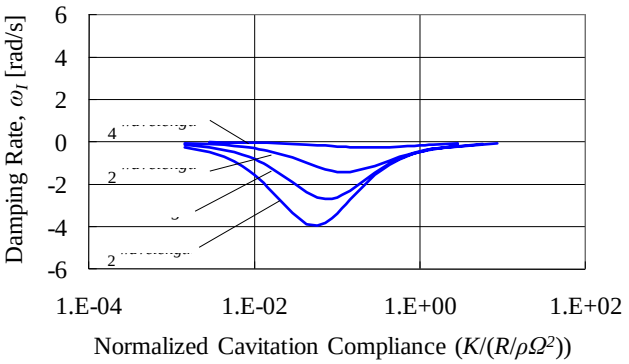

Figure 6(b) ANALYTICAL RESULTS OF IMAGINARY PART, ω_I, SHOWING TREND ANALYSES ON K ($M\rho\Omega$ = 0.035, K_{drag}= 0)

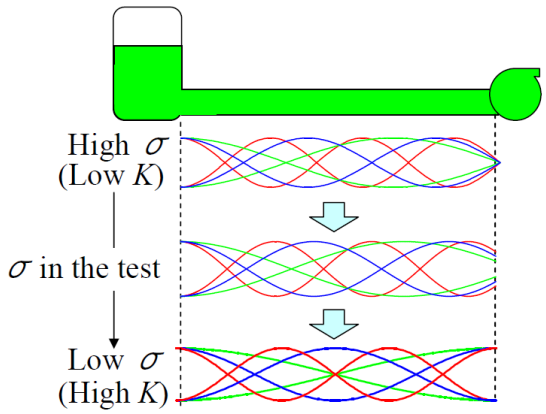

Figure 7 ACOUSTIC MODE IN A FEED PIPE WITH DECREASE OF CAVITATION NUMBER (σ)

THE EFFECT OF PSD

An actual liquid rocket propulsion system is usually equipped with a Pogo suppression device (PSD), which is a kind of surge tank, upstream of a liquid oxidizer turbopump. The purpose of PSD is to avoid Pogo instability, lowering the first characteristics frequency of the inlet pipe to below the structural resonant frequency. To simulate the liquid rocket propulsion system, we installed a PSD in the experimental facility and conducted turbopump tests as illustrated in Fig. 8. The experimental results are shown in Fig. 9. Even if the cavitaion number is decreased, the frequency of cavitation surge remains constant at a certain cavitation number. The frequency then decreases to some extent, but it again remains constant at another cavitation number. These results were different from the experimental results without a PSD in Fig. 2(a) and Fig. 2(b), and thus we modified the analytical model to evaluate the effect of the PSD.

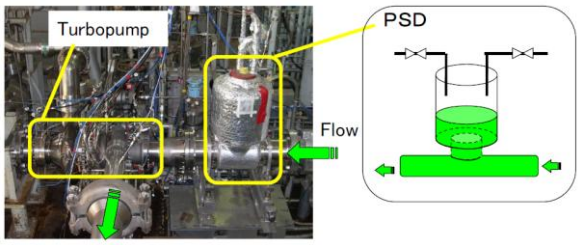

Figure 8 TEST FACILITY WITH POGO SUPPRESSION DEVICE

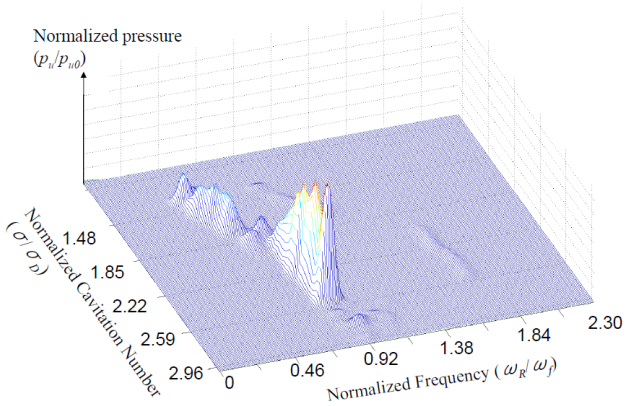

Figure 9(a) FFT ANALYSES OF PRESSURE FLUCTUATION AT INLET OF TURBOPUMP WITH PSD

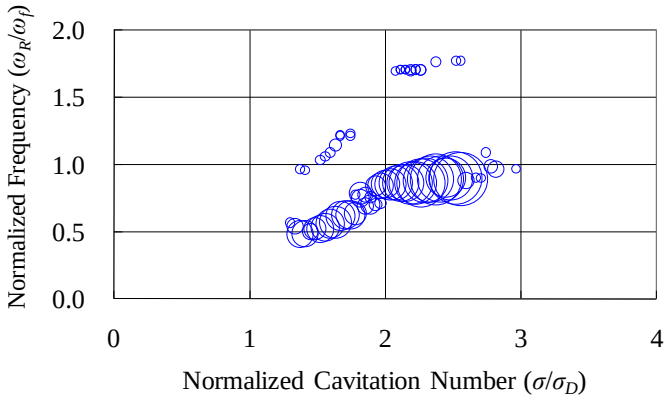

Figure 9(b) EXPERIMENTAL RESULTS OF FLUCTUATING PRESSURE AT THE INLET OF TURBOPUMP WITH PSD

Analytical Model including PSD

The simple analytical model consists of a tank, an inlet pipe, a PSD and a turbopump, as shown in Fig. 10.

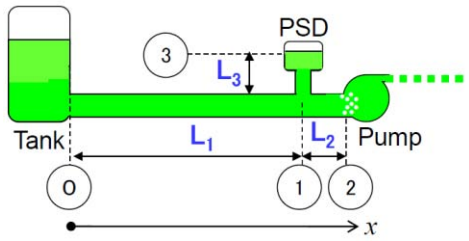

Figure 10 SIMPLE ANALYTICAL MODEL APPLYING PSD

Applying the acoustic wave equation in the pipe between the tank and the PSD (L_1 in Fig. 10), and assuming no drag in the pipe, we obtain Eq. (6)

$$P_{u1} = -j\rho c u_{u1} \tan(\frac{L_1}{c}\omega) \tag{6}$$

Because the length of the PSD (L_3 in Fig. 10) is very short, the inertia motion is applied to this part. In addition, when the suction area of each pipe is assumed to be same for the purposes of simplicity, the unsteady velocities and pressures between the pipe and the PSD (L_3 in Fig. 10) can be expressed in Eq. (7)

$$\begin{aligned} P_{u1} - P_{u3} &= \rho L_3 \dot{u}_{u3} + K_{drag\_PSD}\rho u_{u3} \\ -u_{u3}A &= K_{PSD}\dot{P}_{u3} \end{aligned} \tag{7}$$

The p_{u1} and p_{u3} are eliminated by Eq. (6) and Eq. (7), and then the differential equation on u_{u1} and u_{u3} is obtained.

$$-j\rho c\dot{u}_{u1}\tan(\frac{L_1}{c}\omega) + \frac{A}{K_{PSD}}u_{u3} = \rho L_3 \ddot{u}_{u3} + K_{drag\_PSD}\rho L_3 \dot{u}_{u3} \tag{8}$$

Assuming that u_{u1} and u_{u3} oscillate with the same frequency ($e^{j\omega t}$), we obtain the ratio of $u_{u3} : u_{u1}$ from Eq. (8).

$$S = \frac{u_{u3}}{u_{u1}} = \frac{\omega\rho c \tan(\frac{L_1}{c}\omega_1)}{-\omega^2\rho L_3 + j\omega K_{drag\_PSD}\rho L_3 - \frac{A}{K_{PSD}}} \tag{9}$$

The unsteady velocity u_{u2}, i.e., the unsteady flow rate in the pipe between the PSD and turbopump (L_2 in Fig. 10) is obtained by the difference between u_{u1} and u_{u3}. Then the unsteady pressure and velocity downstream of the branch of the PSD can be expressed by Eq. (10).

$$\begin{aligned} p_{u1} &= P_A(e^{j\omega(t-\frac{L_1}{c})} - e^{j\omega(t+\frac{L_1}{c})}) \\ u_{u1} - u_{u3} &= \frac{P_A}{\rho c}(1-S)(e^{j\omega(t-\frac{L_1}{c})} + e^{j\omega(t+\frac{L_1}{c})}) \end{aligned} \tag{10}$$

On the other hand, general solutions of the acoustic wave equation in the pipe between the PSD and the turbopump (L_2 in Fig. 10) can be obtained by Eq. (11).

$$\begin{aligned} P(t,x) &= P_C e^{j\omega(t-\frac{x-L_1}{c})} + P_D e^{j\omega(t+\frac{x-L_1}{c})} \\ u(t,x) &= \frac{P_C}{\rho c}e^{j\omega(t-\frac{x-L_1}{c})} - \frac{P_D}{\rho c}e^{j\omega(t+\frac{x-L_1}{c})} \end{aligned} \tag{11}$$

When $x = L_1$, Eq. (10) and Eq. (11) become the same value. Hence, two coefficients of P_A, P_C and P_D can be eliminated and Eq. (12) is obtained where $P_D / P_C = T$.

$$\begin{aligned} P_{u2} &= -j\rho c u_{u2}\tan(\frac{L_2}{c}\omega + \beta) \\ \text{where} \quad \cos(\beta) &= \frac{T-1}{\sqrt{4T}}j, \quad \sin(\beta) = \frac{T+1}{\sqrt{4T}} \end{aligned} \tag{12}$$

The characteristic equation on u_{u2} is obtained by Eq. (12) and Eq. (3), and then the solutions of the complex frequency ($\omega = \omega_R + j\omega_I$) can be calculated.

Analytical Results including PSD and Discussion

A comparison between the experimental results and the analytical results, using quasi-steady cavitation compliance (K) and mass flow gain factor (M) mentioned above, is shown in Fig. 11. In the analytical results, when the cavitaion number is decreased, the frequency of the cavitation surge remains constant to a certain cavitation number. The frequency then decreases to some extent, but it again remains constant at another cavitation number. Although there is a small disagreement with the cavitation number, the analytical results qualitatively correspond with the experimental results.

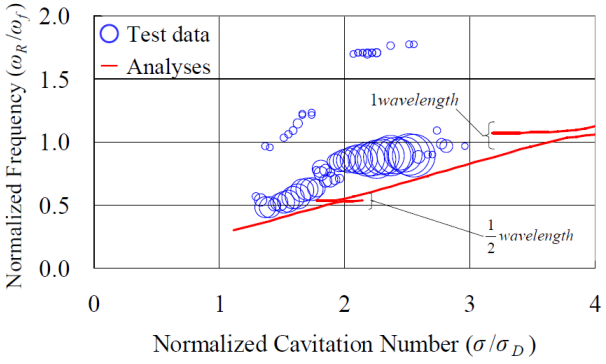

Figure 11 COMPARISON OF FREQUENCY BETWEEN EXPERIMENTAL RESULTS INCLUDING PSD AND ANALYTICAL RESULTS USING CFD-CALCULATED *K* AND *M*

Figure 12 shows the solutions of the frequency of cavitation surge (ω_R) when cavitation compliance (K) is treated as a parameter. When cavitation compliance (K) increases, i.e., the cavitation number decreases, the frequency decreases disconnectedly. Although the cavitation surge without a PSD becomes unstable over a wide range of cavitation compliance (K) (Fig. 6(a)), the cavitation surge with the PSD only becomes unstable when the Helmholtz frequency between the turbopump and the PSD, plotted with broken red line in Fig. 12, coincide with one of the acoustic modes of the pipe. In short, Helmholtz oscillation between the turbopump and the PSD resonates with acoustic modes of the pipe between the tank and the PSD as shown in Fig. 13. The analytical results indicate that the frequency of the cavitation surge basically decreases along the Helmholtz frequency between the turbopump and the PSD with the decrease in cavitation number. When the frequency of the cavitation surge coincides with one of the acoustic modes of the pipe, the frequency remains relatively constant.

Consequently, it is found that when the PSD is installed upstream in the turbopump, the frequency of cavitation surge becomes dependent on the Helmholtz frequency determined by the cavitation compliance (K) of the turbopump and the length between the turbopump and the PSD. And when the frequency coincides with one of the acoustic resonances of the pipe, the cavitation surge resonates and maintains its frequency within a certain range of cavitation number.

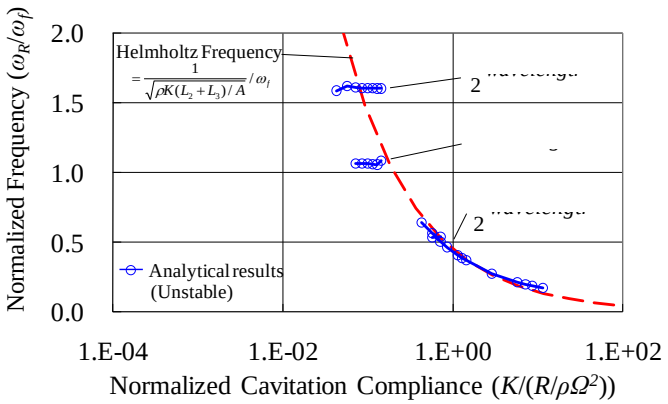

Figure 12 ANALYTICAL RESULTS ON PSD APPLYING MODEL OF REAL PART, ω_R SHOWING TREND ANALYSES ON K ($M\rho\Omega$ = 0.035, K_{drag_PSD}= 0)

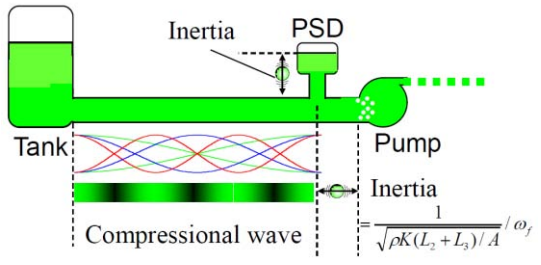

Figure 13 ACOUSTIC MODE IN FEED PIPE WITH PSD

CONCLUSION

To explain the cavitation surge phenomenon in which frequency changes disconnectedly, we conducted the simple one-dimensional analyses by applying an acoustic model. The following points were clarified:

(1) The frequency of cavitation surge decreased disconnectedly with the decrease in cavitation number in turbopump tests. The current analytical model, which uses an inertia model, does not explain this phenomenon. Therefore, we took the factor of compression of the fluid into account and examined the acoustic model. The analytical results then qualitatively corresponded with the experimental results.

(2) The unsteady characteristic of cavitation in the inducer causes pressure fluctuation in which the frequency is determined by acoustic resonance in the inlet pipe and cavitation compliance (K). In this analytical model, the turbopump performs as an intermediate boundary condition between open and closed states because of the characteristic of the cavitation. As the inlet pressure decreases, the characteristic of the inducer changes from a closed boundary condition to an open boundary condition, and then the frequency of the cavitation surge slightly decreases.

(3) When a PSD is installed in the inlet pipe, the frequency of cavitation surge becomes dependent on the Helmholtz frequency between the turbopump and the PSD. And when the cavitation surge resonates with the acoustic modes of the pipe between the tank and the PSD, the frequency remains relatively constant even though the cavitation number is decreased. These analytical results qualitatively corresponded with the experimental results.

In the present study, we conducted linear analyses but did not discuss the nonlinear effect. In the near future, we will investigate this phenomenon by applying nonlinear methods, i.e., finite element methods or a method of characteristics.

ACKNOWLEGEMENT

The authors wish to acknowledge the support of Mr. Koichi Okita, Mr. Syuusuke Hori and Dr. Tomoyuki Hashimoto. We appreciate the assistance in the experiment received from IHI Corporation and Mitsubishi Heavy Industries, LTD.

REFERENCES

[1] Rubin, S., 1966, "Longitudinal Instability of Liquid Rockets Due to Propulsion Feedback (POGO)," *Journal of Spacecraft and Rockets*, Vol. 3, No. 8, pp. 1188-1195.

[2] Brennen, C.E., Acosta, A.J., 1976, "The Dynamic Transfer Function for a Cavitating Inducer," *ASME Journal of Fluids Engineering*, Vol. 98, No. 2, pp. 182-191.

[3] Greitzer, E.M., 1981, "The Stability of Pumping Systems – The 1980 Freeman Scholar Lecture," *ASME Journal of Fluids Engineering*, Vol. 103, No. 2, pp. 193-242.
[4] Tsujimoto, Y., Kamijo, K., Brennen, C.E., 2001, "Unified Treatment of Flow Instabilities of Turbomahines," *Journal of Propulsion and Power*, Vol. 17, No. 3, pp. 636-643.
[5] Yamamoto, K., 1991, "Instability in a Cavitating Centrifugal Pump," *JSME International Journal*, Series 2, Vol. 34, No. 1, pp. 9-17.
[6] Chen, C., Nicolet, C., Yonezawa, K., Farhat, M., Avellan, F., Tsujimoto, Y., One-Dimensional Analysis of Full Load Draft Tube Surge Considering the Finite Sound Velocity in the Penstock, *International Journal of Fluid Machinery and Systems*, Vol. 2, No. 3(2009), pp. 260-268.
[7] Tani, N., Yamanishi, N., 2006, "Cavitaion Surge Prediction Through Steady CFD," *(in Japanese) Thirteenth Symposium on Cavitation*, 2-3 June 2006, Sapporo, Japan. B2-4 Paper No.17.